DALTON
FULL PAPER

A spectroscopic, electrochemical and structural study of polarizable, dipolar ruthenium(II) arsine complexes as models for chromophores with large quadratic non-linear optical responses

Benjamin J. Coe,*[a] Tim Beyer,[b] John C. Jeffery,[b] Simon J. Coles,[c] Thomas Gelbrich,[c] Michael B. Hursthouse[c] and Mark E. Light[c]

[a] *Department of Chemistry, University of Manchester, Oxford Road, Manchester, UK M13 9PL. E-mail: b.coe@man.ac.uk*
[b] *Department of Chemistry, University of Bristol, Cantock's Close, Bristol, UK BS8 1TS*
[c] *EPSRC X-Ray Crystallography Service, Department of Chemistry, University of Southampton, Highfield, Southampton, UK SO17 1BJ*

Received 25th November 1999, Accepted 24th January 2000

The new series of complex salts *trans*-[$Ru^{II}Cl(pdma)_2L][PF_6]_2$ [pdma = 1,2-phenylenebis(dimethylarsine); L = *N*-methyl-4,4′-bipyridinium (MeQ^+) **2**, *N*-phenyl-4,4′-bipyridinium (PhQ^+) **3**, *N*-(4-acetylphenyl)-4,4′-bipyridinium (4-$AcPhQ^+$) **4**, *N*-(2,4-dinitrophenyl)-4,4′-bipyridinium (2,4-$DNPhQ^+$) **5** or *N*-(2-pyrimidyl)-4,4′-bipyridinium (2-$PymQ^+$) **6**] have been prepared. The known complex salt *trans*-[$Ru^{II}Cl(pdma)_2(4,4'\text{-bpy})]PF_6$ (4,4′-bpy = 4,4′-bipyridine) **1** exhibits an intense $d_\pi(Ru^{II})\rightarrow\pi^*$(4,4′-bpy) metal-to-ligand charge-transfer (MLCT) absorption with λ_{max} at 418 nm in acetonitrile, whilst **2**–**6** display $d_\pi(Ru^{II})\rightarrow\pi^*$(L) MLCT bands with λ_{max} values in the region 486–544 nm. The MLCT energy decreases as the electron-accepting ability of L increases, in the order L = $MeQ^+ < PhQ^+ <$ 4-$AcPhQ^+ <$ 2,4-$DNPhQ^+ <$ 2-$PymQ^+$. Cyclic voltammetric studies show that within the series **2**–**6**, the energy of the Ru-based HOMO is almost constant, whilst that of the L-based LUMO decreases by *ca.* 0.4 eV moving from **2** to **6**. Single-crystal structures of the complete series **1**·DMF, **2**, **3**·MeCN, **4**·Me_2CO, **5**·MeCN and **6** have been determined. Analysis of bond lengths and dihedral angles provides no evidence for ground state charge-transfer, despite the strongly dipolar, polarizable nature of these complexes.

Introduction

It is widely anticipated that future optoelectronic and photonic devices will be based upon molecular compounds which exhibit nonlinear optical (NLO) properties.[1] Recent fundamental research into such materials has included studies on organotransition metal complexes which can display very pronounced NLO effects, combined with various other properties such as redox/magnetic behaviour.[2] The elucidation of detailed structure–activity relationships for first hyperpolarizabilities β, which govern molecular quadratic NLO effects, is a major objective of current work with such metal-based chromophores.[3]

The quadratic NLO properties of ruthenium complexes have been investigated in some detail, attention focusing on mixed-valence species,[4] $[Ru^{II}(bpy)_3]^{2+}$ derivatives (bpy = 2,2′-bipyridine),[5] and organometallic σ-acetylide or allenylidene complexes.[6–9] These feature Ru^{II} electron donor centres in combination with various electron acceptor groups. Our studies on dipolar Ru^{II} tetra/penta-ammines with *N*-R-4,4′-bipyridinium (R = Me or aryl) acceptors have shown that such complexes can possess very large quadratic NLO responses.[10] These complexes exhibit intense, low energy metal-to-ligand charge-transfer (MLCT) absorptions, and both the MLCT and NLO properties can be tuned by judicious changes in ligand structure and reversibly switched *via* $Ru^{III/II}$ redox.[11]

Owing to continual difficulties in growing single crystals suitable for X-ray diffraction studies, we have obtained only limited structural information on our dipolar ammine complexes.[10a,c,d] We hence sought to prepare analogous complexes with a different Ru^{II} centre, with the primary objective of gaining detailed crystallographic data. Inspired by previous work with complexes of 1,2-phenylenebis(dimethylarsine) (pdma),[12] we chose to prepare and study a series of complexes featuring *trans*-$\{Ru^{II}Cl(pdma)_2\}^+$ centres co-ordinated to our 4,4′-bipyridinium ligands. The syntheses and properties of these complexes are reported herein.

Experimental

Materials and procedures

The compound $RuCl_3\cdot 2H_2O$ was supplied by Johnson Matthey plc. The salts $[PhQ^+]Cl\cdot 2H_2O$,[10c] [4-$AcPhQ^+$]$Cl\cdot 2H_2O$,[10c] [2,4-$DNPhQ^+$]$PF_6\cdot 0.5H_2O$,[10c] [2-$PymQ^+$]PF_6,[10d] *trans*-[$Ru^{II}Cl(pdma)_2(NO)][PF_6]_2$[13] and *trans*-[$Ru^{II}Cl(pdma)_2(4,4'\text{-bpy})]PF_6$[12b] **1** were prepared according to published procedures. All other reagents were obtained commercially and used as supplied. All reactions were carried out under argon and products were dried overnight at room temperature in a vacuum desiccator ($CaSO_4$) prior to characterization.

Physical measurements

Proton NMR spectra were recorded on a Varian Gemini 200 spectrometer and all shifts are referenced to $SiMe_4$. The fine splitting of pyridyl or phenyl ring AA′BB′ patterns is ignored and the signals are reported as simple doublets, with *J* values referring to the two most intense peaks. Elemental analyses were performed by the Microanalytical Laboratory, University of Manchester. IR spectra were obtained as KBr discs with an ATI Mattson Genesis Series FTIR instrument, and UV/VIS spectra were recorded by using a Hewlett-Packard 8452A diode array spectrophotometer. Mass spectra were recorded by using +electrospray on a Micromass Platform spectrometer (cone

voltage 80 V) (for $[PhQ^+]PF_6$ and $[4\text{-}AcPhQ^+]PF_6$) and +FAB on a Kratos Concept spectrometer with a 6–8 keV Xe atom beam and 3-nitrobenzyl alcohol as matrix (for **2**–**6**).

Cyclic voltammetric measurements were carried out by using an EG&G PAR model 173 potentiostat/galvanostat with a model 175 universal programmer. An EG&G PAR K0264 single-compartment microcell was used with a Ag–AgCl reference electrode (3 M NaCl, saturated AgCl), a platinum-disc working electrode and platinum-wire auxiliary electrode. Acetonitrile (HPLC grade) was used as received and tetra-*n*-butylammonium hexafluorophosphate, twice recrystallized from ethanol and dried *in vacuo*, as supporting electrolyte. Solutions containing *ca.* 10^{-3} mol dm^{-3} analyte (0.1 mol dm^{-3} electrolyte) were deaerated by purging with N_2. All $E_{1/2}$ values were calculated from $(E_{pa} + E_{pc})/2$ at a scan rate of 200 mV s^{-1}.

Syntheses

***N*-Phenyl-4,4′-bipyridinium hexafluorophosphate, $[PhQ^+]PF_6$.** $[PhQ^+]Cl{\cdot}2H_2O$ (346 mg, 1.14 mmol) was dissolved in water (10 cm^3) and aqueous NH_4PF_6 was added dropwise. The cream-coloured precipitate was filtered off, washed with water and dried: yield 395 mg (92%). $\delta_H(CD_3COCD_3)$ 9.52 (2 H, d, *J* 7.1, C_5H_4N–Ph), 8.93 (2 H, br d, C_5H_4N), 8.84 (2 H, d, *J* 7.1, C_5H_4N–Ph), 8.09 (2 H, d, *J* 6.2, C_5H_4N), 8.05–8.00 (2 H, Ph), 7.84–7.81 (3 H, Ph) (Found: C, 50.78; H, 3.11; N, 7.30. Calc. for $C_{16}H_{13}F_6N_2P$: C, 50.81; H, 3.46; N, 7.41%). *m*/*z*: 233 ($[M - PF_6^-]^+$).

***N*-(4-Acetylphenyl)-4,4′-bipyridinium hexafluorophosphate, $[4\text{-}AcPhQ^+]PF_6$.** $[4\text{-}AcPhQ^+]Cl{\cdot}2H_2O$ (360 mg, 1.04 mmol) was dissolved in water (10 cm^3) and aqueous NH_4PF_6 was added dropwise. The golden-brown precipitate was filtered off, washed with water and dried: yield 309 mg (71%). $\delta_H(CD_3COCD_3)$ 9.59 (2 H, d, *J* 7.1, C_5H_4N–C_6H_4COMe), 8.93 (2 H, d, *J* 6.2, C_5H_4N), 8.88 (2 H, d, *J* 7.1, C_5H_4N–C_6H_4COMe), 8.39 (2 H, d, *J* 9.0, C_6H_4), 8.19 (2 H, d, *J* 8.9, C_6H_4), 8.10 (2 H, d, *J* 6.1, C_5H_4N), 2.73 (3 H, s, Me). ν(C=O) 1682s cm^{-1} (Found: C, 51.61; H, 3.51; N, 6.54. Calc. for $C_{18}H_{15}F_6N_2OP$: C, 51.44; H, 3.60; N, 6.67%). *m*/*z*: 275 ($[M - PF_6^-]^+$).

***trans*-$[Ru^{II}Cl(pdma)_2(MeQ^+)][PF_6]_2$ 2.** A solution of **1** (62 mg, 0.061 mmol) in DMF (1.5 cm^3) and methyl iodide (0.5 cm^3) was stirred at room temperature for 32 h. The excess methyl iodide was removed *in vacuo* and addition of aqueous NH_4PF_6 to the deep red solution afforded a dark precipitate which was filtered off, washed with water and dried. Purification was effected by reprecipitation from acetone–diethyl ether followed by recrystallization from acetonitrile–diethyl ether to afford dark red crystals: yield 60 mg (83%). $\delta_H(CD_3COCD_3)$ 9.07 (2 H, d, *J* 6.9, C_5H_4N–Me), 8.41 (2 H, d, *J* 6.9, C_5H_4N–Me), 8.33 (4 H, m, $2C_6H_2$), 7.94 (2 H, d, *J* 6.9, C_5H_4N), 7.85 (4 H, m, $2C_6H_2$), 7.65 (2 H, d, *J* 6.9, C_5H_4N), 4.54 (3 H, s, C_5H_4N–*Me*), 1.92 (12 H, s, 4AsMe), 1.81 (12 H, s, 4AsMe) (Found: C, 31.82; H, 3.93; N, 2.38. Calc. for $C_{31}H_{43}As_4ClF_{12}N_2P_2Ru$: C, 31.83; H, 3.70; N, 2.39%). *m*/*z*: 1024 ($[M - PF_6^-]^+$), 879 ($[M - 2PF_6^-]^+$), 708 ($[M - 2PF_6^- - MeQ^+]^+$).

***trans*-$[Ru^{II}Cl(pdma)_2(PhQ^+)][PF_6]_2$ 3.** A solution of *trans*-$[Ru^{II}Cl(pdma)_2(NO)][PF_6]_2$ (75 mg, 0.073 mmol) and NaN_3 (4.9 mg, 0.075 mmol) in acetone (5 cm^3) was stirred at room temperature for 2 h. Butan-2-one (10 cm^3) and $[PhQ^+]PF_6$ (138 mg, 0.365 mmol) were added and the acetone was removed *in vacuo*. The solution was heated under reflux for 2 h, then evaporated to dryness and the residue was dissolved in acetone (*ca.* 4 cm^3). The slow addition of aqueous NH_4PF_6 afforded a sticky, dark precipitate which was filtered off, washed with water and dried. The product was dissolved in acetone, filtered to remove a small amount of insoluble material, and precipitated by the slow addition of diethyl ether to afford a deep red solid film: yield 58 mg (65%). $\delta_H(CD_3COCD_3)$ 9.37 (2 H, d, *J* 7.2, C_5H_4N–Ph), 8.58 (2 H, d, *J* 7.1, C_5H_4N–Ph), 8.34 (4 H, m, $2C_6H_2$), 7.98 (2 H, d, *J* 6.9, C_5H_4N), 7.91–7.84 (6 H, $2C_6H_2$ and Ph), 7.77–7.71 (5 H, Ph and C_5H_4N), 1.93 (12 H, s, 4AsMe), 1.83 (12 H, s, 4AsMe) (Found: C, 35.05; H, 3.73; N, 2.23. Calc. for $C_{36}H_{45}As_4ClF_{12}N_2P_2Ru$: C, 35.10; H, 3.68; N, 2.27%). *m*/*z*: 1086 ($[M - PF_6^-]^+$), 941 ($[M - 2PF_6^-]^+$), 708 ($[M - 2PF_6^- - PhQ^+]^+$).

***trans*-$[Ru^{II}Cl(pdma)_2(4\text{-}AcPhQ^+)][PF_6]_2$ 4.** This was prepared and purified in an identical manner to **3** by using $[4\text{-}AcPhQ^+]PF_6$ (154 mg, 0.366 mmol) in place of $[PhQ^+]PF_6$. A deep red solid film was obtained: yield 60 mg (65%). $\delta_H(CD_3COCD_3)$ 9.43 (2 H, d, *J* 6.9, C_5H_4N–C_6H_4COMe), 8.61 (2 H, d, *J* 7.0, C_5H_4N–C_6H_4COMe), 8.36–8.29 (6 H, C_6H_4COMe and $2C_6H_2$), 8.04 (2 H, d, *J* 8.8, C_6H_4COMe), 8.00 (2 H, d, *J* 7.0, C_5H_4N), 7.86 (4 H, m, $2C_6H_2$), 7.74 (2 H, d, *J* 6.9, C_5H_4N), 2.69 (3 H, s, C(O)Me), 1.93 (12 H, s, 4AsMe), 1.83 (12 H, s, 4AsMe). ν(C=O) 1686s cm^{-1} (Found: C, 35.71; H, 3.96; N, 2.16. Calc. for $C_{38}H_{47}As_4ClF_{12}N_2OP_2Ru$: C, 35.83; H, 3.72; N, 2.20%). *m*/*z*: 1128 ($[M - PF_6^-]^+$), 983 ($[M - 2PF_6^-]^+$), 708 ($[M - 2PF_6^- - 4\text{-}AcPhQ^+]^+$).

***trans*-$[Ru^{II}Cl(pdma)_2(2,4\text{-}DNPhQ^+)][PF_6]_2$ 5.** This was prepared and purified in an identical manner to **3** by using $[2,4\text{-}DNPhQ^+]PF_6{\cdot}0.5H_2O$ (171 mg, 0.358 mmol) in place of $[PhQ^+]PF_6$. A deep purple microcrystalline solid was obtained: yield 56 mg (56%). $\delta_H(CD_3COCD_3)$ 9.41 (2 H, d, *J* 7.0, C_5H_4N–$C_6H_3(NO_2)_2$), 9.22 (1 H, d, *J* 2.4, H^3), 8.98 (1 H, dd, *J* 2.5, 8.7, H^5), 8.72 (2 H, d, *J* 7.1, C_5H_4N–$C_6H_3(NO_2)_2$), 8.44 (1 H, d, *J* 8.8, H^6), 8.34 (4 H, m, $2C_6H_2$), 8.03 (2 H, d, *J* 6.9, C_5H_4N), 7.86 (4 H, m, $2C_6H_2$), 7.78 (2 H, d, *J* 6.9, C_5H_4N), 1.93 (12 H, s, 4AsMe), 1.84 (12 H, s, 4AsMe). $\nu_{as}(NO_2)$ 1547s, $\nu_s(NO_2)$ 1344s cm^{-1} (Found: C, 33.95; H, 3.73; N, 3.95. Calc. for $C_{36}H_{43}As_4ClF_{12}N_4O_4P_2Ru{\cdot}C_3H_6O$: C, 33.94; H, 3.58; N, 4.06%). *m*/*z*: 1176 ($[M - PF_6^-]^+$), 1031 ($[M - 2PF_6^-]^+$), 708 ($[M - 2PF_6^- - 2,4\text{-}DNPhQ^+]^+$). The acetone of crystallization was detected as a singlet at δ 2.09, and a ν(C=O) band at 1714 cm^{-1}.

***trans*-$[Ru^{II}Cl(pdma)_2(2\text{-}PymQ^+)][PF_6]_2$ 6.** This was prepared and purified in an identical manner to **3** by using $[2\text{-}PymQ^+]PF_6$ (139 mg, 0.366 mmol) in place of $[PhQ^+]PF_6$. A deep purple solid was obtained: yield 56 mg (62%). $\delta_H(CD_3COCD_3)$ 10.22 (2 H, d, *J* 7.4, C_5H_4N–$C_4N_2H_3$), 9.21 (2 H, d, *J* 4.8, $H^{4,6}$), 8.69 (2 H, d, *J* 7.5, C_5H_4N–$C_4N_2H_3$), 8.35 (4 H, m, $2C_6H_2$), 8.03 (2 H, d, *J* 7.0, C_5H_4N), 7.98 (1 H, t, *J* 4.8, H^5), 7.87 (4 H, m, $2C_6H_2$), 7.79 (2 H, d, *J* 7.0, C_5H_4N), 1.93 (12 H, s, 4AsMe), 1.84 (12 H, s, 4AsMe) (Found: C, 33.45; H, 3.59; N, 4.52. Calc. for $C_{34}H_{43}As_4ClF_{12}N_4P_2Ru$: C, 33.10; H, 3.51; N, 4.54%). *m*/*z*: 1088 ($[M - PF_6^-]^+$), 943 ($[M - 2PF_6^-]^+$), 708 ($[M - 2PF_6^- - 2\text{-}PymQ^+]^+$).

X-Ray structural determinations

Crystals of salts **2**, **3**·MeCN, **5**·MeCN and **6** were obtained by slow diffusion of diethyl ether vapour into acetonitrile solutions. Crystals of **1**·DMF and **4**·Me_2CO were grown similarly by using DMF or acetone, respectively. The crystals chosen for diffraction studies had the following appearances and approximate dimensions: **1**·DMF (yellow plate, 0.275 × 0.05 × 0.01 mm), **2** (red block, 0.4 × 0.4 × 0.15 mm), **3**·MeCN (red plate, 0.10 × 0.10 × 0.03 mm), **4**·Me_2CO (red plate, 0.125 × 0.075 × 0.01 mm), **5**·MeCN (brown prism, 0.25 × 0.15 × 0.15 mm), **6** (purple plate, 0.30 × 0.10 × 0.01 mm).

In **1**·DMF a solvent molecule was detected but could not be resolved, so was removed from the dataset using experimental software. In each of **2**, **3**·MeCN and **5**·MeCN, one of the two PF_6^- anions is disordered and the other in **2** is made up of two PF_6^-/2 fragments occupying special positions. The crystals of **6**

Table 1 Crystallographic data and refinement details for salts **1**·DMF, **2**, **3**·MeCN, **4**·Me_2CO, **5**·MeCN and **6**

	1·DMF	**2**	**3**·MeCN	**4**·Me_2CO	**5**·MeCN	**6**
Formula	$C_{30}H_{40}As_4ClF_6N_2PRu$	$C_{31}H_{43}As_4ClF_{12}N_2P_2Ru$	$C_{38}H_{48}As_4ClF_{12}N_3P_2Ru$	$C_{41}H_{53}As_4ClF_{12}N_2O_2P_2Ru$	$C_{38}H_{46}As_4ClF_{12}N_5O_4P_2Ru$	$C_{34}H_{43}As_4ClF_{12}N_4P_2Ru$
M	1009.81	1169.81	1272.93	1331.99	1362.94	1233.86
Crystal system	Monoclinic	Monoclinic	Monoclinic	Orthorhombic	Triclinic	Monoclinic
Space group	$P2_1/c$	$P2_1/c$	$P2_1/c$	$Pna2_1$	$P\bar{1}$	$P2_1/c$
a/Å	17.847(4)	20.273(3)	15.2797(5)	14.519(3)	12.1453(4)	20.2099(8)
b/Å	9.386(2)	9.518(4)	17.1152(6)	22.552(5)	13.7579(4)	9.1355(5)
c/Å	27.936(6)	23.9254(9)	19.3725(6)	16.361(3)	15.7162(5)	25.8443(12)
α/°					108.745(2)	
β/°	101.44(3)	115.057(10)	111.127(2)		95.169(2)	110.886(3)
γ/°					90.339(2)	
U/Å^3	4586.6(17)	4182(2)	4725.7(3)	5357.1(19)	2474.97(13)	4458.0(4)
Z	4	4	4	4	2	4
T/K	150(2)	293(2)	150(2)	150(2)	150(2)	150(2)
μ/mm^{-1}	3.342	3.736	3.315	2.930	3.178	3.511
Reflections collected	18799	25532	22745	47991	22636	26158
Independent reflections (R_{int})	5811 (0.1061)	9516 (0.0241)	8360 (0.0737)	11521 (0.1613)	8695 (0.0675)	7870 (0.1415)
Final $R1$, $wR2$ [$I > 2\sigma(I)$][a]	0.0727, 0.1663	0.0219, 0.0445	0.0464, 0.0903	0.0547, 0.1143	0.0459, 0.0965	0.1238, 0.3157
(all data)	0.1257, 0.1881	0.0320, 0.0472	0.0976, 0.1011	0.1323, 0.1498	0.0871, 0.1070	0.1885, 0.3401

[a] Structures were refined on F_o^2 using all data; the value of $R1$ is given for comparison with older refinements based on F_o with a typical threshold of $F_o > 4\sigma(F_o)$.

twin as multiple stacks; the reported poor quality structure is the best result from a number of datasets. Restraints were applied to the thermal parameters of the following atoms to prevent them from going non-positive definite; N4, C18, C28 and C33. Crystallographic data and refinement details are presented in Table 1.

CCDC reference number 186/1821.

See http://www.rsc.org/suppdata/dt/a9/a909336b/ for crystallographic files in .cif format.

Results and discussion

Synthesis and characterisation

The MeQ^+-containing complex salt **2** was prepared in high yield simply by methylation of the free 4,4′-bipyridine nitrogen atom in the salt **1**.[12b] The salts **3**–**6** were synthesised in good yields from the precursor *trans*-$[Ru^{II}Cl(pdma)_2(NO)][PF_6]_2$,[13] by using a previously developed procedure which involves nucleophilic attack by azide ion on the linearly bonded nitrosyl ligand,[12] followed by reaction of the resulting dinitrogen complex with the PF_6^- salt of the appropriate *N*-(aryl)-4,4′-bipyridinium ligand.

The proton NMR spectrum of each new complex salt exhibits a characteristic AA′BB′ pattern for the eight phenylene ring protons and two singlets for the 24 $AsMe_2$ protons, confirming the presence of a *trans*-$\{Ru^{II}(pdma)_2\}^{2+}$ centre. Signals for the 4,4′-bipyridinium ligands are also observed, and these generally shift downfield as the ligands become more electron deficient. For example, the doublets for the 2,6-protons of the pyridinium rings reveal the deshielding order MeQ^+ < PhQ^+ < 2,4-DNPhQ^+ ≤ 4-AcPhQ^+ < 2-PymQ^+, with a difference of 1.15 ppm between the two extremes.

Electronic spectroscopy studies

Electronic absorption spectra for the new complex salts were recorded in acetonitrile and results are presented in Table 2, together with data for the related $\{Ru^{II}(NH_3)_5\}^{2+}$ salts for purposes of comparison.[10c,d] The complexes in **2**–**6** all show intense, broad $d_\pi(Ru^{II}) \rightarrow \pi^*(L)$ (L = 4,4′-bipyridinium ligand) metal-to-ligand charge-transfer (MLCT) bands with λ_{max} in the region 486–544 nm. The energies of these absorptions depend on the relative energies of the Ru-based HOMO and of the L-based LUMO.[10,14] By contrast with **2**–**6**, the MLCT band in **1** is found at rather higher energy ($\lambda_{max} = 418$ nm, $\varepsilon = 8400$ dm^3 mol^{-1}

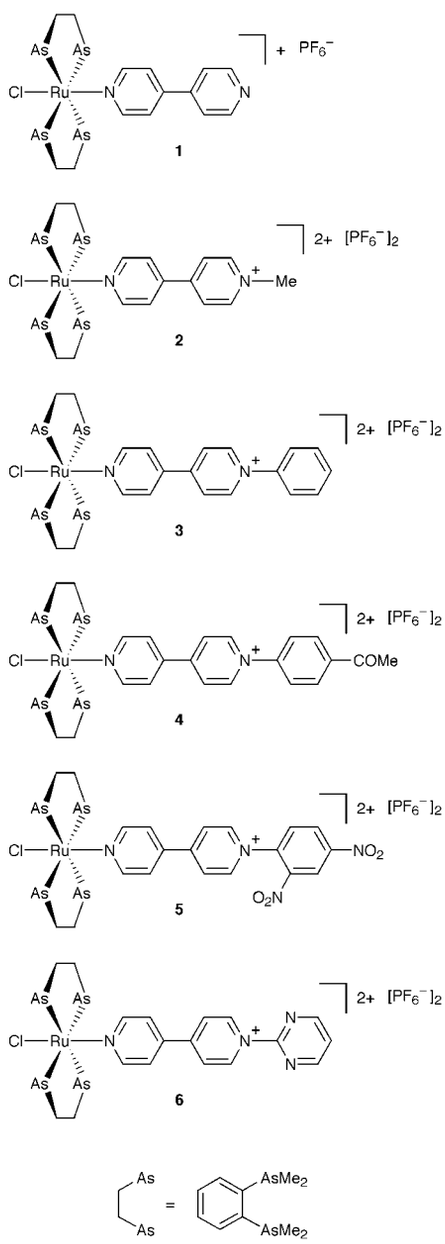

Table 2 Electrochemical and MLCT absorption data in acetonitrile

Complex salt	$E_{1/2}$ V *vs.* Ag–AgCl (ΔE_p/mV)[a]			λ_{max}[MLCT]/nm[b] (ε/dm^3 mol^{-1} cm^{-1})	E_{max}[MLCT]/eV
	$Ru^{III/II}$	$L^{+/0}$	$L^{0/-}$		
2 *trans*-$[Ru^{II}Cl(pdma)_2(MeQ^+)][PF_6]_2$	1.14 (70)	−0.74 (80)	−1.28 (80)	486 (8300)	2.55
3 *trans*-$[Ru^{II}Cl(pdma)_2(PhQ^+)][PF_6]_2$	1.15 (80)	−0.58 (80)	−1.13 (85)	510 (12 500)	2.43
4 *trans*-$[Ru^{II}Cl(pdma)_2(4\text{-}AcPhQ^+)][PF_6]_2$	1.15 (85)	−0.51 (90)	−1.00 (75)	520 (10 000)	2.38
5 *trans*-$[Ru^{II}Cl(pdma)_2(2,4\text{-}DNPhQ^+)][PF_6]_2$	1.16 (85)	−0.38[c]		536 (10 400)	2.31
6 *trans*-$[Ru^{II}Cl(pdma)_2(2\text{-}PymQ^+)][PF_6]_2$	1.16 (80)	−0.34 (90)	−0.98 (80)	544 (10 400)	2.28
$[Ru^{II}(NH_3)_5(MeQ^+)][PF_6]_3$[d]	0.48 (75)	−0.89 (70)	−1.50 (70)	590 (15 800)	2.10
$[Ru^{II}(NH_3)_5(PhQ^+)][PF_6]_3$[d]	0.48 (75)	−0.73 (70)	−1.33 (70)	628 (19 300)	1.97
$[Ru^{II}(NH_3)_5(4\text{-}AcPhQ^+)][PF_6]_3$[d]	0.49 (80)	−0.62 (75)	−1.15 (155)[g]	654 (18 000)	1.90
$[Ru^{II}(NH_3)_5(2,4\text{-}DNPhQ^+)][PF_6]_3$[d]	0.48[e]	−0.38[c]		660 (16 900)	1.88
$[Ru^{II}(NH_3)_5(2\text{-}PymQ^+)][PF_6]_3$[f]	0.51 (100)	−0.43 (200)[g]		673 (18 000)	1.84

[a] Measured in solutions *ca.* 10^{-3} mol dm^{-3} in analyte and 0.1 mol dm^{-3} in $NBu^n_4PF_6$ at a platinum-bead/disc working electrode with a scan rate of 200 mV s^{-1}. Ferrocene internal reference $E_{1/2}$ = 0.43 V, ΔE_p = 90 mV. [b] Solutions 5–7 × 10^{-5} mol dm^{-3}. [c] E_{pc} for an irreversible reduction process. [d] Ref. 10(*c*). [e] E_{pa} for an irreversible oxidation process. [f] Ref. 10(*d*). [g] Irreversible process as evidenced by $i_{pc} \neq i_{pa}$.

cm^{-1}),[12b] owing to the weaker electron-accepting ability of 4,4′-bpy compared with the 4,4′-bipyridinium ligands. Each of the complexes in **3**, **4** and **6** also shows one intense UV absorption (λ_{max} *ca.* 285 nm, ε = 20–25 × 10^3 dm^3 mol^{-1} cm^{-1}) owing to intraligand $\pi \longrightarrow \pi^*$ excitations.

The steady red-shifting of the MLCT bands in **2**–**6** indicates that the acceptor strength of L increases (*i.e.* the LUMO energy decreases) in the order $MeQ^+ < PhQ^+ < 4\text{-}AcPhQ^+ < 2,4\text{-}DNPhQ^+ < 2\text{-}PymQ^+$. This parallels the trend observed in the analogous pentaammine complexes.[10c,d] The total MLCT energy shift in moving from MeQ^+ to $2\text{-}PymQ^+$ is also the same in both series of complexes (0.26–0.27 eV). The blue-shift of the MLCT bands on replacing a $\{Ru^{II}(NH_3)_5\}^{2+}$ with a *trans*-$\{Ru^{II}Cl(pdma)_2\}^+$ centre is roughly constant at 0.43–0.48 eV, indicating that the latter is a considerably weaker electron donor, *i.e.* has a lower HOMO energy. The MLCT extinction coefficients in **2**–**6** are also considerably smaller than those of their pentaammine counterparts, showing that d_π/π^*-orbital overlap is more efficient in the latter complexes.

Electrochemical studies

The new complex salts were studied by cyclic voltammetry in acetonitrile and results are presented in Table 2, together with data for the related $\{Ru^{II}(NH_3)_5\}^{2+}$ salts.[10c,d] The complexes in **2**–**4** and **6** exhibit reversible $Ru^{III/II}$ oxidation waves, together with two reversible ligand-based reduction processes, whilst in **5** only the $Ru^{III/II}$ wave is reversible.

The $Ru^{III/II}$ $E_{1/2}$ values for **2**–**6** are shifted by +650–670 mV with respect to those of their pentaammine analogues,[10c,d] confirming that the *trans*-$\{Ru^{II}Cl(pdma)_2\}^+$ centre is much less electron rich than $\{Ru^{II}(NH_3)_5\}^{2+}$, as indicated by the MLCT data (see earlier). In both series of complexes, changing L has a negligible effect on the HOMO energy. The electronic difference between the two Ru^{II} centres is also detected in the L first reduction potentials which reveal that the ligands are more easily reduced (by 90–150 mV), and hence more electron-deficient, in **2**–**6** than in their $\{Ru^{II}(NH_3)_5\}^{2+}$ counterparts. However, this decrease in the LUMO energies is more than offset by the decreased HOMO energies, leading to the higher MLCT energies for **2**–**6** (see earlier). The L first reduction potentials in **2**–**6** confirm that the electron acceptor strength increases in the order $MeQ^+ < PhQ^+ < 4\text{-}AcPhQ^+ < 2,4\text{-}DNPhQ^+ < 2\text{-}PymQ^+$, with a decrease in the LUMO energy of *ca.* 0.4 eV moving from **2** to **6**.

Crystallographic studies and relevance to NLO properties

Single crystal X-ray structures were obtained for **1**·DMF, **2**, **3**·MeCN, **4**·Me_2CO, **5**·MeCN and **6**. Representations of the molecular structures of the complex cations are shown in Figs. 1–6, respectively, and selected interatomic distances and angles are presented in Table 3.

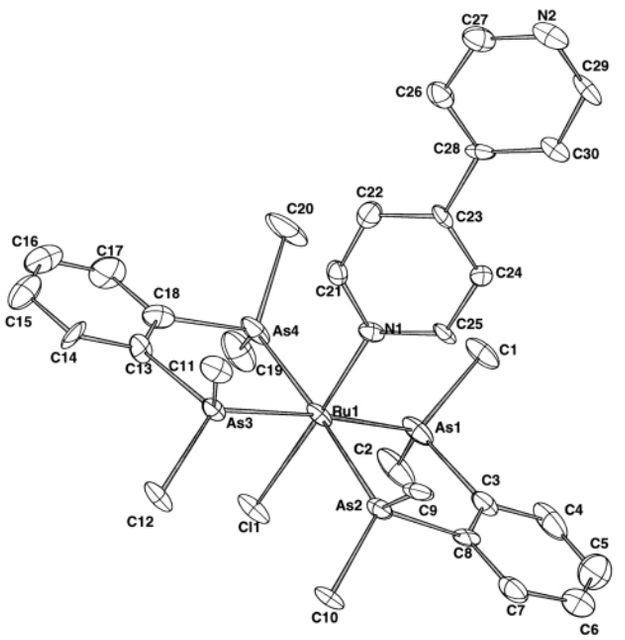

Fig. 1 Structural representation of the complex cation in the salt **1**·DMF (50% probability ellipsoids).

We have previously found that the 4,4′-bpy ligand in *trans*-$[Ru^{II}(NH_3)_4py(4,4'\text{-}bpy)][PF_6]_2$·2MeCN is twisted, with an inter-ring torsion angle of 38.5°.[10d] The comparable angles in *trans*-$[Ru^{II}(NH_3)_4(MeQ^+)(PTZ)][PF_6]_3$·$Me_2CO$[10a] (PTZ = phenothiazine) and *trans*-$[Ru^{II}(NH_3)_4(PhQ^+)(PTZ)][PF_6]_3$·$Et_2O$[10c] are 9.6 and 2.6°, respectively. We suggested that these data indicate increased Ru^{II}–ligand delocalization in the latter two complexes owing to the greater electron-withdrawing abilities of MeQ^+ and PhQ^+ with respect to 4,4′-bpy.[10d] The primary purpose of the present study was to test this hypothesis, the expectation being that $Ru^{II} \longrightarrow L$ polarization will increase with the electron accepting strength of L in the order $MeQ^+ < PhQ^+ < 4\text{-}AcPhQ^+ < 2,4\text{-}DNPhQ^+ < 2\text{-}PymQ^+$, leading to increased planarity and quinoidal structure of the 4,4′-bipyridinium unit.

Examination of the data in Table 3 reveals that the dihedral angle between the pyridyl rings (angle 1) increases in the order **1**·DMF ≤ **6** ≤ **3**·MeCN < **5**·MeCN < **2** < **4**·Me_2CO, showing no correlation with the ligand acceptor strength. Furthermore, neither the C–C distances between the pyridyl rings nor the N(pyridinium)–C(aryl) distances show any trend or evidence of

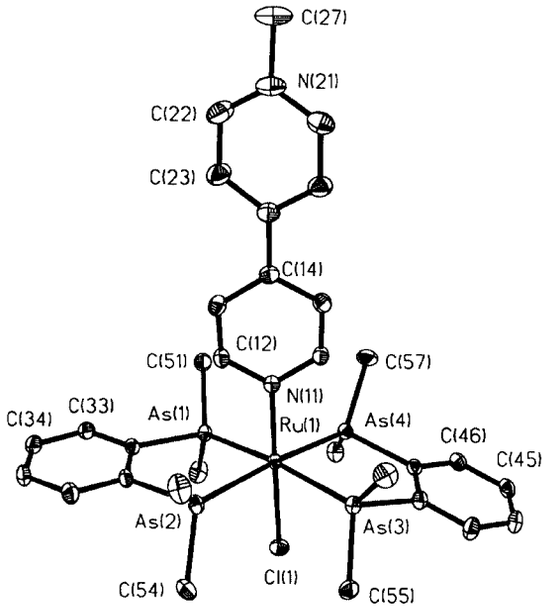

Fig. 2 Structural representation of the complex cation in the salt **2** (50% probability ellipsoids).

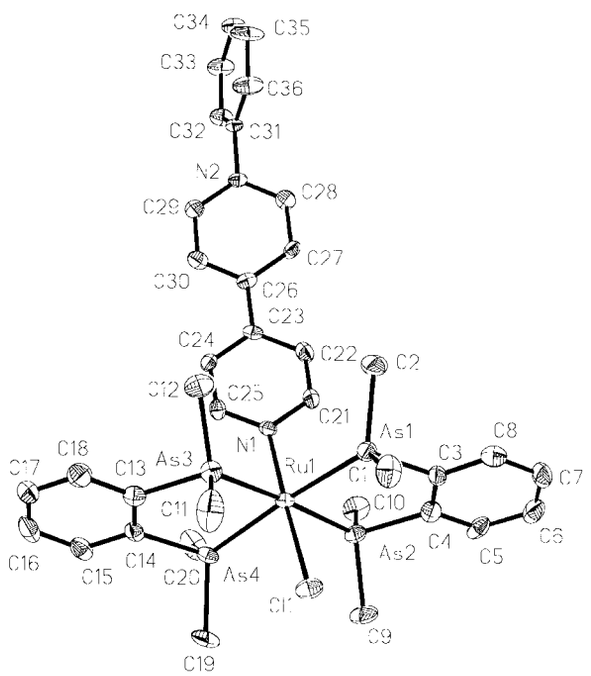

Fig. 3 Structural representation of the complex cation in the salt **3**·MeCN (50% probability ellipsoids).

partial double bond character, and the 4,4′-bpy rings are fully aromatic in all cases. There is clearly no significant charge transfer in the ground states of these complexes. On reflection, this observation is consistent with the electrochemical data which show that changing the *N*-substituent in L does not significantly affect the energy of the Ru-based HOMO (see earlier). It can hence be concluded that the torsion angle differences observed in the related tetraammine complexes are not due to electronic effects, but are simply caused by crystal packing factors.

One further point of interest concerns the 2,4-DNPhQ$^+$ complex in **5**·MeCN. We have previously found that the static molecular first hyperpolarizability β_0 of the related complex in $[Ru^{II}(NH_3)_5(2,4\text{-}DNPhQ^+)][PF_6]_3$ appears to be smaller than that of $[Ru^{II}(NH_3)_5(4\text{-}AcPhQ^+)][PF_6]_3$.[10c] It was suggested that this may be caused by a steric effect whereby the *ortho*-NO_2

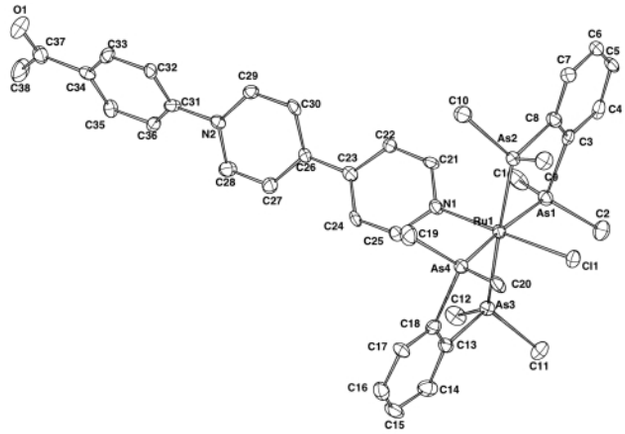

Fig. 4 Structural representation of the complex cation in the salt **4**·Me_2CO (50% probability ellipsoids).

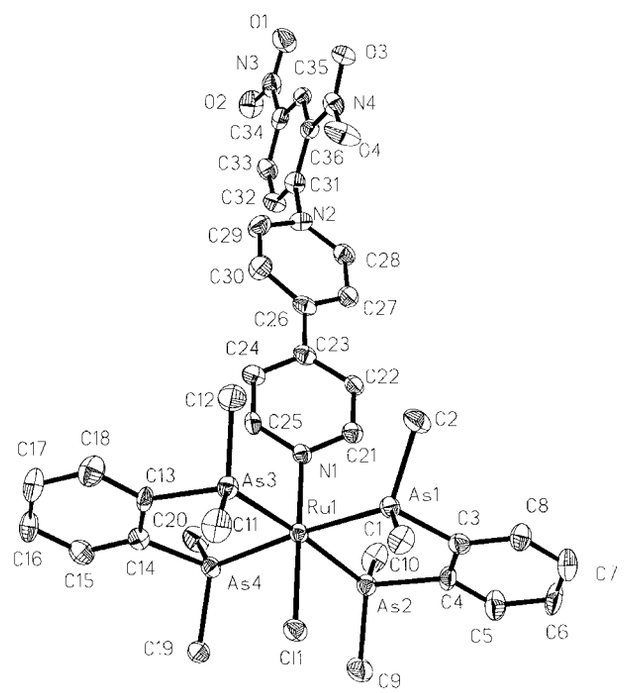

Fig. 5 Structural representation of the complex cation in the salt **5**·MeCN (50% probability ellipsoids).

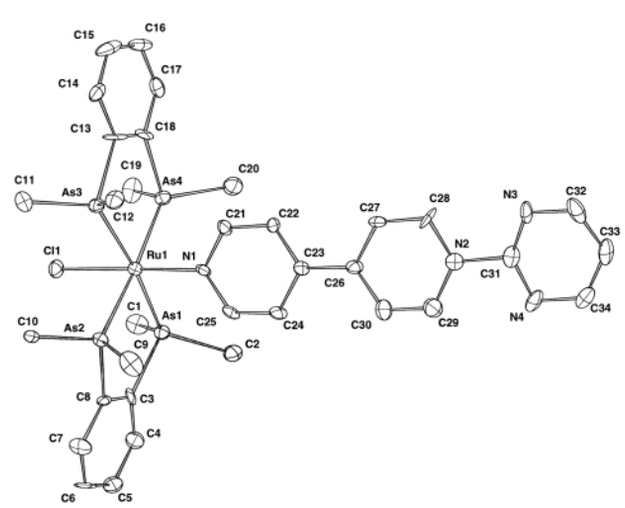

Fig. 6 Structural representation of the complex cation in the salt **6** (50% probability ellipsoids).

Table 3 Selected interatomic distances (Å) and angles (°) for salts **1**·DMF, **2**, **3**·MeCN, **4**·Me_2CO, **5**·MeCN and **6**

	1·DMF	**2**	**3**·MeCN	**4**·Me_2CO	**5**·MeCN	**6**
Ru1–As1	2.424(6)	2.4174(6)	2.4300(7)	2.4587(11)	2.4213(7)	2.432(3)
Ru1–As2	2.421(6)	2.4257(4)	2.4268(7)	2.4958(12)	2.4233(7)	2.416(3)
Ru1–As3	2.423(6)	2.4292(5)	2.4114(7)	2.4986(12)	2.4155(7)	2.421(3)
Ru1–As4	2.410(7)	2.4245(5)	2.4108(7)	2.4499(12)	2.4184(7)	2.419(3)
Ru1–Cl1	2.455(12)	2.4292(7)	2.4255(14)	2.436(2)	2.4207(12)	2.420(6)
Ru1–N11/N1	2.10(3)	2.104(2)	2.095(4)	2.093(8)	2.089(4)	2.097(18)
inter-ring C–C distance[a]	1.53(6)	1.489(3)	1.483(7)	1.467(13)	1.485(7)	1.49(3)
N21–C27/N2–C31		1.480(3)	1.460(6)	1.464(11)	1.447(6)	1.53(3)
As1–Ru1–As2	84.2(2)	84.69(2)	85.28(2)	87.64(4)	85.30(2)	84.70(10)
As1–Ru1–As3	173.6(2)	171.046(11)	94.93(2)	95.06(4)	93.97(2)	171.27(11)
As1–Ru1–As4	94.4(2)	92.99(2)	173.94(3)	173.33(5)	173.96(2)	94.91(10)
As1–Ru1–Cl1	87.6(3)	87.59(3)	85.55(4)	85.44(7)	86.78(4)	85.03(16)
As1–Ru1–N11/N1	93.5(10)	94.04(5)	93.05(12)	93.2(2)	93.59(11)	94.3(5)
As2–Ru1–As3	95.4(2)	96.22(2)	175.48(3)	175.57(5)	174.35(2)	94.84(10)
As2–Ru1–As4	174.8(2)	172.516(11)	95.45(2)	90.36(4)	94.68(2)	174.83(12)
As2–Ru1–Cl1	88.9(4)	87.44(2)	86.44(4)	86.84(7)	85.60(4)	85.97(17)
As2–Ru1–N11/N1	93.3(10)	92.15(5)	91.86(11)	92.8(2)	94.01(12)	93.3(5)
As3–Ru1–As4	85.4(2)	84.98(2)	83.86(2)	86.57(4)	85.45(2)	84.77(10)
As3–Ru1–Cl1	86.0(3)	83.55(3)	89.07(4)	89.87(7)	88.76(4)	86.24(17)
As3–Ru1–N11/N1	92.9(10)	94.82(5)	92.64(11)	90.6(2)	91.63(12)	94.4(5)
As4–Ru1–Cl1	86.0(4)	85.35(2)	88.49(4)	88.10(7)	87.19(3)	88.86(17)
As4–Ru1–N11/N1	91.8(10)	95.11(5)	92.94(12)	93.2(2)	92.44(11)	91.8(5)
Cl1–Ru1–N11/N1	177.6(12)	178.27(5)	177.88(12)	178.6(2)	179.45(11)	179.1(5)
Dihedral angle 1[b]	10.27(5)	23.91(2)	15.1(2)	25.04(3)	20.0(2)	10.85(1.30)
Dihedral angle 2[c]			69.7(2)	42.57(4)	84.5(1)	8.53(1.26)

[a] For **1**·DMF = C23–C28; for **2** = C14–C24; for **3**·MeCN, **4**·Me_2CO, **5**·MeCN and **6** = C23–C26. [b] Angles between planes defined by atoms as follows: for **1**·DMF, **3**·MeCN, **4**·Me_2CO, **5**·MeCN and **6**, N1–C21–C22–C23–C24–C25 and N2–C26–C27–C28–C29–C30; for **2**, N11–C12–C13–C14–C15–C16 and N21–C22–C23–C24–C25–C26. [c] Angles between planes defined by atoms as follows: for **3**·MeCN, **4**·Me_2CO and **5**·MeCN, N2–C26–C27–C28–C29–C30 and C31–C32–C33–C34–C35–C36; for **6**, N2–C26–C27–C28–C29–C30 and C31–N3–C32–C33–C34–N4.

group reduces the likelihood of the phenyl ring becoming coplanar with the 4,4′-bipyridinium unit.[10c] Hence, the electron-withdrawing influence of the 2,4-DNPh ring will be almost solely inductive in nature. By contrast, in the 4-AcPhQ$^+$ complex, no steric hindrance exists, and the ability to adopt a coplanar conformation may allow the 4-AcPh ring to exert both inductive and mesomeric electron-withdrawing effects. The structure of **5**·MeCN provides evidence in support of this postulate since the pyridinium and 2,4-DNPh rings are almost perpendicular, with a dihedral angle of 84.5(1)°. We have also recently observed similar effects in the *trans*-4′-(dimethylamino)-*N*-(2,4-dinitrophenyl)-4-stilbazolium cation.[15]

Although they have polarizable, dipolar structures, we have chosen not to investigate the quadratic NLO properties of the new complexes in **2**–**6** for two reasons. Firstly, the MLCT absorption and electrochemical data clearly show that the *trans*-{$Ru^{II}Cl(pdma)_2$}$^+$ centre is a considerably less effective electron donor than {$Ru^{II}(NH_3)_5$}$^{2+}$ (see earlier). Hence, the β_0 values of **2**–**6** will be smaller than those of their pentaammine analogues. Secondly, the MLCT bands of **2**–**6** lie very close to 532 nm, precluding the acquisition of meaningful hyper-Rayleigh scattering[16] data with a standard 1064 nm Nd–YAG laser fundamental. Nevertheless, it is anticipated that **2**–**6** will exhibit substantial quadratic NLO activities. It is therefore noteworthy that all of the new complex salts adopt centrosymmetric space groups, with the exception of **4**·Me_2CO. The space group $Pna2_1$ belongs to the point group *mm*2 which is one of only four suitable for optimal efficiency of second harmonic generation (SHG),[17] a macroscopic quadratic NLO effect. A crystal packing diagram of **4**·Me_2CO reveals that the complex dipoles (as represented by the Ru1–N2 vectors) form an angle θ_m of 34.7° with the polar *c* axis (Fig. 7). The ideal value of θ_m for SHG in *mm*2 symmetry is 54.7°.[17]

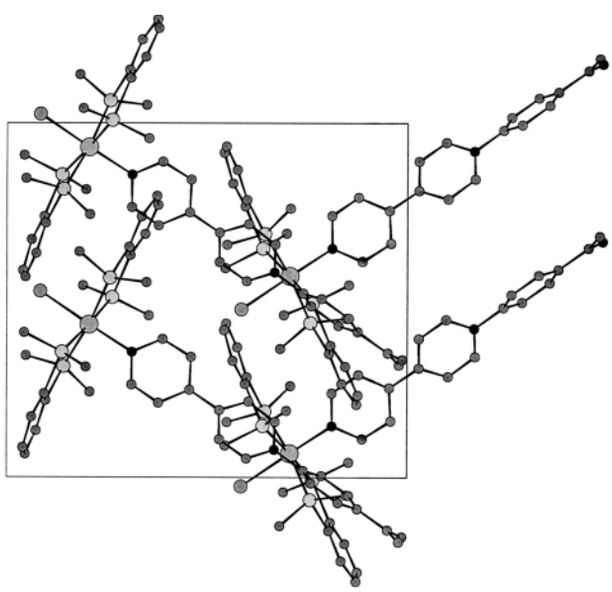

Fig. 7 Crystal packing diagram of the complex cations in the salt **4**·Me_2CO (view along *b* axis).

Conclusion

MLCT absorption and electrochemical data for complexes of *N*-R-4,4′-bipyridinium (R = Me or aryl) ligands show that the *trans*-{$Ru^{II}Cl(pdma)_2$}$^+$ centre is a considerably less effective electron donor than {$Ru^{II}(NH_3)_5$}$^{2+}$. Analysis of bond lengths and dihedral angles obtained from X-ray structural studies on a series of *trans*-{$Ru^{II}Cl(pdma)_2$}$^+$ complex salts provides no evidence for ground state charge transfer, despite the strongly dipolar, polarizable nature of the complexes.

Acknowledgements

This work was supported by a research grant from The Royal Society. Thanks are due to Johnson Matthey plc for a generous loan of ruthenium trichloride.

References

1 *Nonlinear Optical Properties of Organic Molecules and Crystals*, ed. D. S. Chemla and J. Zyss, Academic Press, Orlando, FL, 1987, vols. 1 and 2; J. Zyss, *Molecular Nonlinear Optics: Materials, Physics and Devices*, Academic Press, Boston, 1994; S. R. Marder, B. Kippelen, A. K.-Y. Jen and N. Peyghambarian, *Nature*, 1997, **388**, 845; T. Verbiest, S. Houbrechts, M. Kauranen, K. Clays and A. Persoons, *J. Mater. Chem.*, 1997, **7**, 2175.

2 S. R. Marder, in *Inorganic Materials*, ed. D. W. Bruce and D. O'Hare, Wiley, Chichester, 1992; D. R. Kanis, M. A. Ratner and T. J. Marks, *Chem. Rev.*, 1994, **94**, 195; N. J. Long, *Angew. Chem., Int. Ed. Engl.*, 1995, **34**, 21; I. R. Whittall, A. M. McDonagh, M. G. Humphrey and M. Samoc, *Adv. Organomet. Chem.*, 1998, **42**, 291.

3 Selected recent examples: S. Barlow, H. E. Bunting, C. Ringham, J. C. Green, G. U. Bublitz, S. G. Boxer, J. W. Perry and S. R. Marder, *J. Am. Chem. Soc.*, 1999, **121**, 3715; I. S. Lee, H. Seo and Y. K. Chung, *Organometallics*, 1999, **18**, 1091; E. Licandro, S. Maiorana, A. Papagni, P. Hellier, L. Capella, A. Persoons and S. Houbrechts, *J. Organomet. Chem.*, 1999, **583**, 111; O. Briel, K. Sünkel, I. Krossing, H. Nöth, E. Schmälzlin, K. Meerholz, C. Bräuchle and W. Beck, *Eur. J. Inorg. Chem.*, 1999, 483; J. Heck, S. Dabek, T. Meyer-Friedrichsen and H. Wong, *Coord. Chem. Rev.*, 1999, **190**–**192**, 1217.

4 W. M. Laidlaw, R. G. Denning, T. Verbiest, E. Chauchard and A. Persoons, *Nature*, 1993, **363**, 58; W. M. Laidlaw, R. G. Denning, T. Verbiest, E. Chauchard and A. Persoons, *Proc. SPIE, Int. Soc. Opt. Eng.*, 1994, **2143**, 14.

5 J. Zyss, C. Dhenaut, T. Chauvan and I. Ledoux, *Chem. Phys. Lett.*, 1993, **206**, 409; C. Dhenaut, I. Ledoux, I. D. W. Samuel, J. Zyss, M. Bourgault and H. Le Bozec, *Nature*, 1995, **374**, 339; F. W. Vance and J. T. Hupp, *J. Am. Chem. Soc.*, 1999, **121**, 4047.

6 I. R. Whittall, M. G. Humphrey, A. Persoons and S. Houbrechts, *Organometallics*, 1996, **15**, 1935; R. H. Naulty, A. M. McDonagh, I. R. Whittall, M. P. Cifuentes, M. G. Humphrey, S. Houbrechts, J. Maes, A. Persoons, G. A. Heath and D. C. R. Hockless, *J. Organomet. Chem.*, 1998, **563**, 137.

7 S. Houbrechts, K. Clays, A. Persoons, V. Cadierno, M. P. Gamasa and J. Gimeno, *Organometallics*, 1996, **15**, 5266; V. Cadierno, S. Conejero, M. P. Gamasa, J. Gimeno, I. Asselberghs, S. Houbrechts, K. Clays, A. Persoons, J. Borge and S. García-Granda, *Organometallics*, 1999, **18**, 582.

8 M. Tamm, T. Jentzsch and W. Werncke, *Organometallics*, 1997, **16**, 1418.

9 I.-Y. Wu, J. T. Lin, J. Luo, S.-S. Sun, C.-S. Li, K. J. Lin, C. Tsai, C.-C. Hsu and J.-L. Lin, *Organometallics*, 1997, **16**, 2038; I.-Y. Wu, J. T. Lin, J. Luo, C.-S. Li, C. Tsai, Y.-S. Wen, C.-C. Hsu, F.-F. Yeh and S. Liou, *Organometallics*, 1998, **17**, 2188.

10 (*a*) B. J. Coe, M. C. Chamberlain, J. P. Essex-Lopresti, S. Gaines, J. C. Jeffery, S. Houbrechts and A. Persoons, *Inorg. Chem.*, 1997, **36**, 3284; (*b*) B. J. Coe, J. P. Essex-Lopresti, J. A. Harris, S. Houbrechts and A. Persoons, *Chem. Commun.*, 1997, 1645; (*c*) B. J. Coe, J. A. Harris, L. J. Harrington, J. C. Jeffery, L. H. Rees, S. Houbrechts and A. Persoons, *Inorg. Chem.*, 1998, **37**, 3391; (*d*) B. J. Coe, J. A. Harris, I. Asselberghs, A. Persoons, J. C. Jeffery, L. H. Rees, T. Gelbrich and M. B. Hursthouse, *J. Chem. Soc., Dalton Trans.*, 1999, 3617.

11 B. J. Coe, S. Houbrechts, I. Asselberghs and A. Persoons, *Angew. Chem., Int. Ed.*, 1999, **38**, 366; B. J. Coe, *Chem. Eur. J.*, 1999, **5**, 2464.

12 (*a*) B. J. Coe, M. Chery, R. L. Beddoes, H. Hope and P. S. White, *J. Chem. Soc., Dalton Trans.*, 1996, 3917; (*b*) B. J. Coe, S. Hayat, R. L. Beddoes, M. Helliwell, J. C. Jeffery, S. R. Batten and P. S. White, *J. Chem. Soc., Dalton Trans.*, 1997, 591.

13 P. G. Douglas, R. D. Feltham and H. G. Metzger, *J. Am. Chem. Soc.*, 1971, **93**, 84.

14 P. Ford, De F. P. Rudd, R. Gaunder and H. Taube, *J. Am. Chem. Soc.*, 1968, **90**, 1187; C. R. Johnson and R. E. Shepherd, *Inorg. Chem.*, 1983, **22**, 2439.

15 B. J. Coe, J. A. Harris, I. Asselberghs, G. Olbrechts, K. Clays, A. Persoons, S. J. Coles and M. B. Hursthouse, results to be published.

16 K. Clays and A. Persoons, *Phys. Rev. Lett.*, 1991, **66**, 2980; *Rev. Sci. Instrum.*, 1992, **63**, 3285; E. Hendrickx, K. Clays and A. Persoons, *Acc. Chem. Res.*, 1998, **31**, 675.

17 J. Zyss and J. L. Oudar, *Phys. Rev. A*, 1982, **26**, 2028.

Paper a909336b